Paradox of inductionless magnetorotational instability

Jānis Priede[1,2], Ilmārs Grants[2], and Gunter Gerbeth[2]
[1]Institute of Physics, University of Latvia, LV–2169 Salaspils, Latvia
[2]Forschungszentrum Rossendorf, MHD Department, P.O. Box 510119, D–01314 Dresden, Germany

E-mail: priede@sal.lv

Abstract. We consider the magnetorotational instability (MRI) of a hydrodynamically stable Taylor-Couette flow with a helical external magnetic field in the inductionless approximation defined by a zero magnetic Prandtl number ($\mathrm{Pm} = 0$). This leads to a considerable simplification of the problem eventually containing only hydrodynamic variables. First, we point out that the energy of any perturbation growing in the presence of magnetic field has to grow faster without the field. This is a paradox because the base flow is stable without the magnetic while it is unstable in the presence of a helical magnetic field without being modified by the latter as it has been found recently by Hollerbach and Rüdiger [Phys. Rev. Lett. **95**, 124501 (2005)]. We revisit this problem by using a Chebyshev collocation method to calculate the eigenvalue spectrum of the linearized problem. In this way, we confirm that MRI with helical magnetic field indeed works in the inductionless limit where the destabilization effect appears as an effective shift of the Rayleigh line. Second, we integrate the linearized equations in time to study the transient behavior of small amplitude perturbations, thus showing that the energy arguments are correct as well. However, there is no real contradiction between both facts. The linear stability theory predicts the asymptotic development of an arbitrary small-amplitude perturbation, while the energy stability theory yields the instant growth rate of any particular perturbation, but it does not account for the evolution of this perturbation. Thus, although switching off the magnetic field instantly increases the energy growth rate, in the same time the critical perturbation ceases to be an eigenmode without the magnetic field. Consequently, this perturbation is transformed with time and so looses its ability to extract energy from the base flow necessary for the growth.

1. Introduction

The magnetorotational instability (MRI) is thought to be responsible for the fast formation of stars and entire galaxies in accretion disks. For a star to form, the matter rotating around it has to slow down by transferring its angular momentum outwards. Without MRI this process would take much longer than observed because the velocity distribution in the accretion disks seems to be hydrodynamically stable while the viscosity alone is not sufficient to account for the actual accretion rates. It was suggested by Balbus and Hawley [1, 2] that a Keplerian velocity distribution in an accretion disk can be destabilized by a magnetic field analogously to a hydrodynamically stable cylindrical Taylor-Couette flow as it was originally found by Velikhov [3] and later analysed in more detail by Chandrasekhar [4]. In this case, the effect of "frowziness" of the axial magnetic field in a well conducting fluid provides an additional coupling between the meridional and azimuthal flow perturbations that, however, requires a magnetic Reynolds number of Rm ~ 10. For a liquid metal with the magnetic Prandtl number Pm $\sim 10^{-5}-10^{-6}$ this corresponds to a hydrodynamic Reynolds number $\mathrm{Re} = \mathrm{Rm}/\mathrm{Pm} \sim 10^6 - 10^7$ [5, 6]. Thus, this instability is hardly observable in the laboratory because any conceivable flow at such Reynolds number would be turbulent. However, it was shown recently by Hollerbach and Rüdiger [7] that MRI can take place in the Taylor-Couette flow at Re $\sim 10^3$ when the imposed magnetic field is helical. The most surprising fact is that this type of MRI persists even in the inductionless limit of Pm $= 0$ where the critical Reynolds number of the conventional MRI diverges as $\sim 1/\mathrm{Pm}$. This limit of Pm $= 0$ formally corresponds to a poorly conducting medium where the induced currents are so weak that their magnetic field is negligible with respect to the imposed field. Thus, on one hand, the imposed magnetic field does not affect the base flow, which is the only source of energy for the perturbation growth. But on the other hand, perturbations are subject to additional damping due to the Ohmic dissipation caused by the induced currents.

We show rigorously that the imposed magnetic field indeed reduces the energy growth rate of any particular perturbation. On one hand, this implies that the energy of any perturbation, which is growing in the presence of magnetic field, has to grow even faster without the field and vice versa. But on the other hand, the flow which is found to be unstable in the presence of magnetic field is certainly known to be stable without the field. This apparent contradiction constitutes the paradox of the inductionless MRI which we address in this study.

The paper is organized as follows. In Section 2, we formulate the problem in the inductionless approximation. Numerical results are presented and discussed in Section 3. The paper is concluded with summary in Section 4.

2. Problem formulation

Consider an incompressible fluid of kinematic viscosity ν and electrical conductivity σ filling the gap between two infinite concentric cylinders with inner radius R_i and outer radius R_o rotating with angular velocities Ω_i and Ω_o, respectively, in the presence of an externally imposed steady magnetic field $\mathbf{B}_0 = B_\phi \mathbf{e}_\phi + B_z \mathbf{e}_z$ with axial and azimuthal components $B_z = B_0$ and $B_\phi = \beta B_0 R_i/r$ in cylindrical coordinates (r, ϕ, z), where β is a dimensionless parameter characterizing the geometrical helicity of the field. Further, we assume the magnetic field of the currents induced by the fluid flow to be negligible relative to the imposed field that corresponds to the so-called inductionless approximation holding for most of liquid-metal magnetohydrodynamics characterized by small magnetic Reynolds numbers $\mathrm{Rm} = \mu_0 \sigma v_0 L \ll 1$, where μ_0 is the magnetic permeability of vacuum, v_0 and L are the characteristic velocity and length scale. The velocity of fluid flow $\mathbf{v}$ is governed by the Navier-Stokes equation with electromagnetic body force

$$\frac{\partial \mathbf{v}}{\partial t} + (\mathbf{v} \cdot \boldsymbol{\nabla})\mathbf{v} = -\frac{1}{\rho}\boldsymbol{\nabla} p + \nu \boldsymbol{\nabla}^2 \mathbf{v} + \frac{1}{\rho}\mathbf{j} \times \mathbf{B}_0, \tag{1}$$

where the induced current follows from Ohm's law for a moving medium

$$\mathbf{j} = \sigma \left(\mathbf{E} + \mathbf{v} \times \mathbf{B}_0\right). \tag{2}$$

In addition, we assume that the characteristic time of velocity variation is much longer than the magnetic diffusion time $\tau_0 \gg \tau_m = \mu_0 \sigma L^2$ that leads to the quasi-stationary approximation, according to which $\boldsymbol{\nabla} \times \mathbf{E} = 0$ and $\mathbf{E} = -\boldsymbol{\nabla}\Phi$, where Φ is the electrostatic potential. Mass and charge conservation imply $\boldsymbol{\nabla} \cdot \mathbf{v} = \boldsymbol{\nabla} \cdot \mathbf{j} = 0$.

The problem admits a base state with a purely azimuthal velocity distribution $\mathbf{v}_0(r) = \mathbf{e}_\phi v_0(r)$, where

$$v_0(r) = r\frac{\Omega_o R_o^2 - \Omega_i R_i^2}{R_o^2 - R_i^2} + \frac{1}{r}\frac{\Omega_o - \Omega_i}{R_o^{-2} - R_i^{-2}}.$$

Note that the magnetic field does not affect the base flow because it gives rise only to the electrostatic potential $\Phi_0(r) = B_0 \int v_0(r)dr$ whose gradient compensates the induced electric field so that there is no current in the base state ($\mathbf{j}_0 = 0$). However, a current may appear in a perturbed state

$$\left\{ \begin{array}{c} \mathbf{v}, p \\ \mathbf{j}, \Phi \end{array} \right\} (\mathbf{r}, t) = \left\{ \begin{array}{c} \mathbf{v}_0, p_0 \\ \mathbf{j}_0, \Phi_0 \end{array} \right\} (r) + \left\{ \begin{array}{c} \mathbf{v}_1, p_1 \\ \mathbf{j}_1, \Phi_1 \end{array} \right\} (\mathbf{r}, t)$$

where $\mathbf{v}_1$, p_1, $\mathbf{j}_1$, and Φ_1 present small-amplitude perturbations for which Eqs. (1, 2) after linearization take the form

$$\begin{aligned} \frac{\partial \mathbf{v}_1}{\partial t} + (\mathbf{v}_1 \cdot \boldsymbol{\nabla})\mathbf{v}_0 + (\mathbf{v}_0 \cdot \boldsymbol{\nabla})\mathbf{v}_1 &= -\frac{1}{\rho}\boldsymbol{\nabla} p_1 + \nu \boldsymbol{\nabla}^2 \mathbf{v}_1 + \frac{1}{\rho}\mathbf{j}_1 \times \mathbf{B}_0 \qquad (3) \\ \mathbf{j}_1 &= \sigma \left(-\boldsymbol{\nabla}\Phi_1 + \mathbf{v}_1 \times \mathbf{B}_0 \right). \qquad (4) \end{aligned}$$

In the following, we focus on axisymmetric perturbations, which are typically much more unstable than non-axisymmetric ones [8]. In this case, the solenoidity constraints are satisfied by meridional stream functions for fluid flow and electric current as

$$\mathbf{v} = v\mathbf{e}_\phi + \boldsymbol{\nabla} \times (\psi \mathbf{e}_\phi), \qquad \mathbf{j} = j\mathbf{e}_\phi + \boldsymbol{\nabla} \times (h\mathbf{e}_\phi).$$

Note that h is the azimuthal component of the induced magnetic field which is used subsequently as an alternative to Φ for the description of the induced current. In addition, for numerical purposes, we introduce also the vorticity $\boldsymbol{\omega} = \omega \mathbf{e}_\phi + \boldsymbol{\nabla} \times (v\mathbf{e}_\phi) = \boldsymbol{\nabla} \times \mathbf{v}$ as an auxiliary variable. Then the perturbation may be sought in the normal mode form

$$\{v_1, \omega_1, \psi_1, h_1\} (\mathbf{r}, t) = \left\{ \hat{v}, \hat{\omega}, \hat{\psi}, \hat{h} \right\} (r) \times e^{\gamma t + ikz},$$

where γ is in general a complex growth rate and k is the axial wave number. Henceforth, we proceed to dimensionless variables by using R_i, R_i^2/ν, $R_i\Omega_i$, B_0, and $\sigma B_0 R_i \Omega_i$ as the length, time, velocity, magnetic field, and current scales, respectively. The nondimensionalized governing equations read as

$$\begin{aligned} \gamma \hat{v} &= D_k \hat{v} + \mathrm{Re}ik \left(r^2 \Omega \right)' r^{-1} \hat{\psi} + \mathrm{Ha}^2 ik \hat{h}, \qquad (5) \\ \gamma \hat{\omega} &= D_k \hat{\omega} + 2\mathrm{Re}ik\Omega \hat{v} - \mathrm{Ha}^2 ik \left(ik\hat{\psi} + 2\beta r^{-2} \hat{h} \right), \qquad (6) \\ 0 &= D_k \hat{\psi} + \hat{\omega}, \qquad (7) \\ 0 &= D_k \hat{h} + ik \left(\hat{v} - 2\beta r^{-2} \hat{\psi} \right), \qquad (8) \end{aligned}$$

where $D_k f \equiv r^{-1} (rf')' - (r^{-2} + k^2) f$ and the prime stands for d/dr; $\mathrm{Re} = R_i^2 \Omega_i / \nu$ and $\mathrm{Ha} = R_i B_0 \sqrt{\sigma/(\rho\nu)}$ are Reynolds and Hartmann numbers, respectively;

$$\Omega(r) = \frac{\lambda^{-2} - \mu + r^{-2} (\mu - 1)}{\lambda^{-2} - 1}$$

is the dimensionless angular velocity of the base flow defined using $\lambda = R_o/R_i$ and $\mu = \Omega_o/\Omega_i$. Boundary conditions for the flow perturbation on the inner and outer cylinders at $r = 1$ and $r = \lambda$, respectively, are $\hat{v} = \hat{\psi} = \hat{\psi}' = 0$. Boundary conditions for $\hat{h}$ on insulating and perfectly conducting cylinders, respectively, are $\hat{h} = 0$ and $(r\hat{h})' = 0$ at $r = 1; \lambda$.

The governing Eqs. (5–8) for perturbation amplitudes were discretized using a spectral collocation method on a Chebyshev-Lobatto grid with a typical number of internal points $N = 32{-}96$. Auxiliary Dirichlet boundary conditions for $\hat{\omega}$ were introduced and then numerically

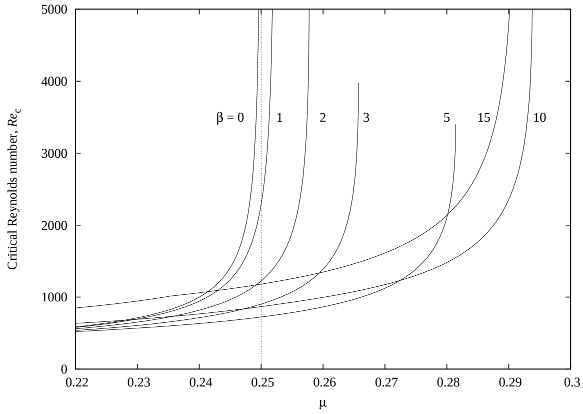

Figure 1. Critical Reynolds number versus μ for insulating cylinders with $\lambda = 2$ at various helicities β and fixed Hartmann number $\mathrm{Ha} = 15$.

eliminated to satisfy the no-slip boundary conditions $\hat{\psi}' = 0$. Electric stream function $\hat{h}$ was expressed in terms of $\hat{v}$ and $\hat{\psi}$ by solving Eq. (8) and then substituted in Eqs. (5, 6) that eventually resulted in the $2N \times 2N$ complex matrix eigenvalue problem which was efficiently solved by the LAPACK's ZGEEV routine.

In addition, Eqs. (5–8) were discretized by using a Chebyshev-tau approximation and integrated forward in time by a fully implicit 2nd order scheme with linear extrapolation of convective and magnetic terms. We tested the numerical code by finding a few leading eigenmodes and eigenvalues by the so-called "snapshot" method [9] and compared to the results of the above described code as well as to the linear instability results [10] and [7]. Agreement was at least three significant digits.

Equations (3, 4) straightforwardly lead to the kinetic energy variation rate of a virtual perturbation $\mathbf{v}_1$ satisfying the incompressiblity constraint and the boundary conditions. Multiplying Eq. (3) scalarly by $\mathbf{v}_1$ and then integrating over the volume V which extends axially over the perturbation wavelength, we obtain

$$\frac{\partial E_1}{\partial t} = -\int \left[\left(\mathbf{v}_1 \cdot \boldsymbol{\nabla} \right) \mathbf{v}_1 \right] \cdot \mathbf{v}_0 dV - \int \left(\nu \boldsymbol{\omega}_1^2 + \frac{\mathbf{j}_1^2}{\sigma} \right) dV,$$

where $E_1 = \frac{1}{2} \int \mathbf{v}_1^2 dV$ is the energy of perturbation. The first integral in the equation above accounts for the interaction of the perturbation with the basic flow which is not affected by the magnetic field as noted above. The sign of this integral may vary depending on $\mathbf{v}_1$. Thus, this term presents a potential source of energy. In contrast, the second term is negative definite presenting an energy sink due to both viscosity and conductivity. Since the current is induced only in the presence of a magnetic field while the source term does not depend on the magnetic field, we conclude that the instant growth rate of any given perturbation has to be lower with magnetic field than without it

$$\left. \frac{\partial E_1}{\partial t} \right|_{B_0 > 0} < \left. \frac{\partial E_1}{\partial t} \right|_{B_0 = 0}. \tag{9}$$

3. Numerical results

The following results concern cylinders with $\lambda = 2$, as in Ref. [7]. As seen in Fig. 1, which shows the critical Reynolds number as a function of μ for Hartmann number $\mathrm{Ha} = 15$ and various geometrical helicities β, the linear instability threshold can indeed extend well beyond

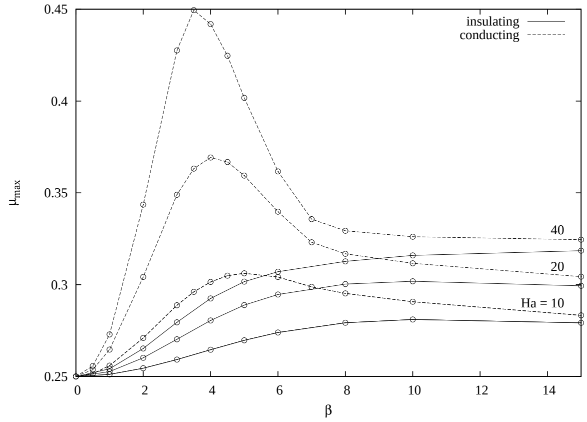

Figure 2. Limiting value of μ versus the helicity β for insulating and perfectly conducting cylinders with $\lambda = 2$ at various Hartmann numbers.

the Rayleigh line $\mu_c = \lambda^{-2} = 0.25$, defined by $d\left(r^2\Omega\right)/dr = 0$, when the magnetic field is helical ($\beta \neq 0$). In contrast to $\mathrm{Pm} \neq 0$ [7], the range of instability is limited by $\mu_{\max}$, which is plotted in Fig. 2 depending on the geometrical helicity β at various Hartmann numbers Ha for both insulating and perfectly conducing cylinders. The critical Re tends to infinity as μ approaches $\mu_{\max}$ as in the nonmagnetic Taylor-Couette instability. Thus, in the inductionless approximation, the destabilizing effect of a helical magnetic field appears as a shift of the Rayleigh line towards higher μ. The shift is especially pronounced for perfectly conducting cylinders at $\beta \approx 4$.

The results of time-integration of the linearized problem are illustrated in Fig. 3 for a perturbation with $k = 2$ at $\mathrm{Re} = 2000$. This perturbation is unstable in the presence of a magnetic field with $\beta = 4$ and $\mathrm{Ha} = 15$ ($\mathrm{Re}_c = 1554$, $k_c = 2.5$) and stable without the field because $\mu = 0.27 > \mu_c$. First, we integrate an arbitrary, sufficiently small initial perturbation for a sufficiently long time so that the unstable mode dominates but still remains small for the linear approximation to be valid. Then we "switch off" the magnetic field by setting $\mathrm{Ha} = 0$. Note that we assume the field to be instantly absent when it is switched off. So we just compare the evolution of the given perturbation with and without the field. As seen on the first inset of Fig. 3, the energy of an unstable perturbation indeed starts to grow faster instantly after the magnetic field is switched off. However, the growth keeps only for a short time and then the energy quickly decays as predicted by the linear stability analysis. Note that the energy keeps decaying in an oscillatory way because the dominating perturbation without the field is not a pure traveling wave but rather a superposition of two oppositely traveling waves which both have the same decay rate and frequency whereas the amplitude ratio of both waves is determined by the initial condition.

The magnetic field is switched on again at the instant $t = 0.1$. The corresponding evolution of the perturbation energy is shown on the r.h.s. of Fig. 3 in enlarged scale. As seen in the second inset, the energy decay rate instantly increases in accordance to (9) when the magnetic field is switched on. However, after a short transient the perturbation energy resumes the growth in agreement with the linear stability analysis. In this case, the energy growth is purely exponential because the dominating perturbation is a single traveling wave. Thus, this particular example of time integration confirms the validity of Eq. (9) which applies in general to any arbitrary perturbation. The energy of an unstable perturbation indeed starts to grow faster when the magnetic field is switched off.

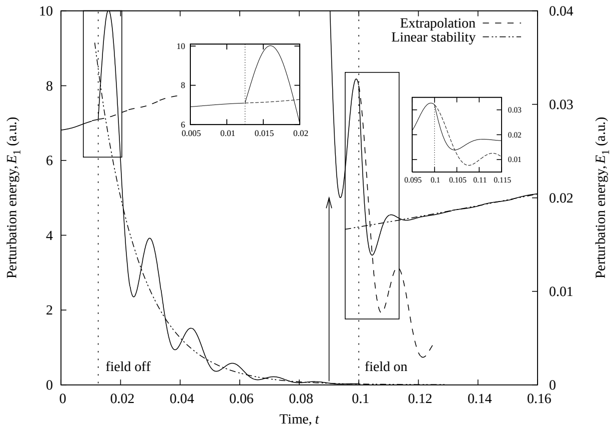

Figure 3. Time evolution of the energy of the dominating perturbation with $k = 2$ at $\mathrm{Re} = 2000$ after switching the magnetic field off and later on again for $\mu = 0.27$, $\mathrm{Ha} = 15$, and $\beta = 4$. Extrapolation shows how the evolution would proceed without the change of the magnetic field.

4. Conclusions

We have considered MRI in the inductionless approximation at $\mathrm{Pm} = 0$ that allowed us to eliminate the magnetic field and, thus, led to a considerable simplification of the problem containing only hydrodynamic variables as in the classical Taylor-Couette problem. First, we used a Chebyshev collocation method to calculate the eigenvalue spectrum of the linearized problem. In this way, we confirmed that MRI with helical magnetic field indeed works in the inductionless limit. Second, we integrated the linearized equations forward in time to study the transient behavior of small amplitude perturbations. In this way, we showed that the energy arguments are correct as well – the energy of an unstable perturbation indeed starts to grow faster when the magnetic field is switched off. However, there is no real contradiction with the linear stability predictions because the energy grows only for a limited time and then turns to decay as predicted by the linear stability. It is important to stress that the linear stability theory predicts the asymptotic development of an arbitrary small-amplitude perturbation, while the energy stability theory yields the instant growth rate of any particular perturbation, but it does not account for the evolution of this perturbation. Thus, although switching off the magnetic field instantly increases the energy growth rate of the most unstable as well as that of any other perturbation, in the same time the critical perturbation ceases to be an eigenmode without the magnetic field. Consequently, this perturbation is transformed with time and so looses its ability to extract energy from the base flow necessary for the growth. Analogously, switching on the magnetic field causes an instant decrease of the growth rate of any particular perturbation because of Ohmic dissipation, while the magnetic field transforms the perturbation so that it becomes able to extract more energy from the base flow and so eventually grows.

To understand the physical mechanism of this instability, note that a helical magnetic field, in contrast to pure axial or azimuthal fields, provides an additional coupling between meridional and azimuthal flow perturbations. In a helical magnetic field with axial and azimuthal components, the radial component of the meridional flow perturbation induces azimuthal and axial current components, respectively. Interaction of this current with the imposed magnetic field results in a purely radial electromagnetic force which retards the original perturbation. So, it has a stabilizing effect similar to the radial deformation of magnetic flux lines in the conventional MRI [3, 4]. However, in the perturbation of finite wavelength there is also a radial current component associated with the axial one as required by the solenoidity constraint. This radial current interacting with the axial component of the helical magnetic field gives rise to the azimuthal electromagnetic force, thus coupling the meridional and azimuthal flow perturbations similarly to the conservation of the angular momentum in the purely hydrodynamic Taylor-Couette instability or the azimuthal twisting of axial magnetic flux lines in the conventional MRI. Note that the latter effect also renders the imposed axial magnetic field locally helical that, however, requires $\mathrm{Pm} > 0$ and $\mathrm{Re} \sim 1/\mathrm{Pm}$.

In conclusion, when the imposed magnetic field is helical, the inductionless approximation defined by $\mathrm{Pm} = 0$ is applicable to MRI where it leads to a considerable simplification of the problem containing only hydrodynamic variables as in the classical Taylor-Couette problem.

Acknowledgments

The research was supported by Deutsche Forschungsgemeinschaft in frame of the Collaborative Research Centre SFB 609. The authors would like to thank G. Rüdiger for helpful comments and discussions.

References

[1] Balbus S A and Hawley J F 1991 *Astrophys. J.* **376** 214
[2] Balbus S A and Hawley J F 1998 *Rev. Mod. Phys.* **70** 1
[3] Velikhov E P 1959 *Sov. Phys. JETP* **36** 995
[4] Chandrasekhar S 1960 *Proc. Nat. Acad. Sci.* **46** 253
[5] Goodman J and Ji H 2002 *J. Fluid. Mech.* **462** 365
[6] Rüdiger G, Schultz M, and Shalybkov D 2003 *Phys. Rev. E.* **67** 046312
[7] Hollerbach R and Rüdiger G 2005 *Phys. Rev. Lett.* **95**, 124501
[8] Rüdiger G, Hollerbach R, Schultz M, and Shalybkov D A 2005 *Astron. Nachr.* **326** 409
[9] Goldhirsch I, Orszag S A, and Maulik B K 1987 *J. Sci. Computing* **2** 33
[10] Chandrasekhar S 1961 *Hydrodynamic and Hydromagnetic Stability* Oxford University, London